

**Rotation of δ Scuti Stars in the Open Clusters
NGC 1817 and NGC 7062¹**

J. Molenda-Żakowicz

Astronomical Institute, University of Wrocław, Kopernika 11, Wrocław, Poland
e-mail: molenda@astro.uni.wroc.pl

T. Arentoft

Department of Physics and Astronomy, Danish AsteroSeismology Center (DASC),
Aarhus University, Ny Munkegade 120, Bldg. 1520, 8000 Århus, Denmark
e-mail: toar@phys.au.dk

S. Frandsen

Department of Physics and Astronomy, Aarhus University, Ny Munkegade 120, Bldg.
1520, 8000 Århus C, Denmark
e-mail: sfr@phys.au.dk

and F. Grundahl

Department of Physics and Astronomy, Aarhus University, Ny Munkegade 120, Bldg.
1520, 8000 Århus C, Denmark
e-mail: fgj@phys.au.dk*Received Month Day, Year*

ABSTRACT

We report results of spectroscopic and photometric observations of ten δ Scuti stars and one eclipsing binary in the open cluster NGC 1817, and of ten δ Scuti stars and two other variables in the open cluster NGC 7062. For all targets in NGC 1817 and for three targets in NGC 7062, the radial velocity and projected rotational velocity are determined. For all stars, the effective temperature and surface gravity is measured.

Two δ Scuti stars, NGC 1817 –V1 and NGC 7062 –V1, and the eclipsing binary, NGC 1817 –V18, are discovered to be single-lined spectroscopic binaries. The eclipsing binary δ Scuti star NGC 1817 –V4 is discovered to be a double-lined spectroscopic binary.

¹Partly based on observations made with the Nordic Optical Telescope, operated on the island of La Palma jointly by Denmark, Finland, Iceland, Norway, and Sweden, in the Spanish Observatorio del Roque de los Muchachos of the Instituto de Astrofísica de Canarias.

All δ Scuti stars which we observed spectroscopically are found to be moderate or fast rotators.

Key words: *Open clusters: NGC 1817, NGC 7062 – Stars: pulsating: δ Scuti – Stars: rotation – Binaries: spectroscopic*

1. Introduction

The δ Scuti-type pulsators are A–F stars with masses between 1.5 and $2.5M_{\odot}$. They oscillate mainly in radial and non-radial p -modes, show light amplitudes at the mmag level and periods of the order of hours. Most δ Scuti stars are multiperiodic which makes them promising targets for asteroseismology because every frequency carries information about the inner structure of the star and therefore, each one provides additional constraints which can be used in tests of stellar models. These tests become more stringent if more parameters can be measured independently as is the case for clusters where one can assume the same age and metallicity for all cluster members in asteroseismic modeling.

A suitable open cluster for a study of δ Scuti variables has an age of 0.3–1.0 Gyr and a distance of 1–2 kpc. This ensures a convenient angular size of the cluster and allows precise photometry of δ Scuti stars, which in this case are found among the cluster’s brightest members. NGC 1817 and NGC 7062 meet these requirements. They are rich in δ Scuti stars (see Arentoft et al. 2005 and Freyhammer et al. 2001) and their angular diameter allows finding the targets in a field of view of a few arc minutes on the sky.

In this paper, we derive the effective temperature and surface gravity of ten δ Scuti stars and one eclipsing binary in NGC 1817, and of ten δ Scuti stars and two other variables in NGC 7062. For all 11 stars in NGC 1817 and for three δ Scuti stars in NGC 7062, we measure the radial velocity and the projected rotational velocity. We plan to use this last parameter, $v \sin i$, as a constraint for target selection in the future multi-site asteroseismic campaigns on δ Scuti stars in these clusters.

This paper is organized as follows. In Section 2, we give an account of our observations and reductions. In Section 3, we determine T_{eff} and $\log g$ of the program stars. In Section 4, we derive the radial velocity and the projected rotational velocity. Section 5 contains a summary.

2. Observations and Reductions

2.1. Photometry of NGC 7062

Strömrgren photometry for NGC 7062 and standard stars were collected at the 2.5-m Nordic Optical Telescope, La Palma, Spain, on three nights in August 2004. Since the third night, 14 August 2004, was non-photometric, it was excluded from the analysis, which is then based on 12 and 13 August 2004. The log of our observations is given in Table 1.

The standard stars were adopted from Olsen (1983, 1984) who provides $uvby - \beta$ magnitudes for stars faint enough to be observed with the NOT. The telescope, however, still had to be defocused in order to avoid very short integration times. The adopted exposure times were 5–40 seconds and, to decrease the dead-time between observations, only a small window of the CCD was read out.

During the observations of NGC 7062, the telescope was in focus and full CCD was read out. The exposure times were 60 s in the y filter, 90 s, in b , 240 s, in v , 1200 s, in u , 120 s, in the narrow β -filter, and 400 s, in the wide.

Table 1

Log of the Strömgen observations of NGC 7062: the numbers of $uvby$ and β sequences and the range in airmass.

Date and object	$uvby$	β	Airmass	Date and object	$uvby$	β	Airmass
12 august 2004				13 August 2004			
Standard stars	18	8	1.01 – 2.15	Standard stars	11	10	1.01 – 1.85
NGC 7062	5	4	1.05 – 1.42	NGC 7062	5	4	1.22 – 1.58

The observations of the standard stars were reduced with aperture photometry. We used the curves of growth to make sure that all photons were included, and we estimated the sky level using the surrounding background. The instrumental $uvby$ -magnitudes for the standard stars were used to derive transformation equations of the form given in Grundahl et al. (2002),

$$y_{obs} = V_{std} + \alpha_y(v - y) + \beta_y(X - 1) + \gamma_y T + \delta_y \quad (1)$$

$$b_{obs} = b_{std} + \alpha_b(v - y) + \beta_b(X - 1) + \gamma_b T + \delta_b \quad (2)$$

$$v_{obs} = v_{std} + \alpha_v(v - y) + \beta_v(X - 1) + \gamma_v T + \delta_v \quad (3)$$

$$u_{obs} = u_{std} + \alpha_u(v - y) + \beta_u(X - 1) + \gamma_u T + \delta_u, \quad (4)$$

where X is the airmass, T , the time of the exposure, and $(v - y)$, the color index in the standard system. The transformation equations were derived on a nightly basis.

The extinction coefficients for the narrow and wide H_β filters were computed from the observations of standard stars for each night separately, and used to calculate the average extinction coefficient, k_β . Then, the total fluxes measured for standard stars were expressed in the units of flux per second, converted to magnitudes and corrected for extinction according to the following equations

$$H_{n,0} = H_{n,obs} - k_\beta X \quad (5)$$

$$H_{w,0} = H_{w,obs} - k_\beta X \quad (6)$$

where X is the airmass, and $H_{n,obs}$ and $H_{w,obs}$, magnitudes in the narrow and wide H_β filter, respectively. Finally, the transformation equation was derived,

$$\beta_{std} = \alpha\beta_0 + \delta \quad (7)$$

where $\beta_0 = H_{w,0} - H_{n,0}$.

In Table 2, we give the standard deviation of the residuals resulting from subtracting the magnitudes of the standard stars transformed with equations 1–4, m_{trans} , from the standard magnitudes, m_{std} , and the standard deviations of the residuals of $\beta_{std} - \beta_{trans}$. The values show that our transformations yield magnitudes which are accurate typically to better than 1%. Furthermore, in the residuals no trends with airmass, color or time are present.

Table 2

Standard deviations of the residuals, $m_{std} - m_{trans}$, computed for $-uvby - \beta$ observations of standard stars (in mmag).

Date	σ_y	σ_b	σ_v	σ_u	σ_β
12 August 2004	4.4	3.0	7.4	7.7	10.8
13 August 2004	6.0	5.4	5.1	13.7	9.4

The photometric reductions of the images of NGC 7062 were done with the software package MOMF (Kjeldsen & Frandsen 1992) which uses a combined PSF and aperture photometry. In this package the size of the aperture is specified by the user. We used MOMF for detecting stars in the images and for deriving the stellar fluxes. When computing the fluxes for stars in NGC 7062, we used smaller apertures than those used for standard stars because of the crowding in the field of the cluster. For isolated cluster stars, we used the curves of growth to verify that the chosen apertures were large enough to include all the photons coming from the star and, at the same time, small enough to protect against undesirable crowding effects.

We transformed the instrumental magnitudes to the standard system using the equations 1–4 and 7. This transformation was done iteratively on a nightly basis. For each star, the first estimate of $(v - y)_{std}$ was calculated from all measurements on a given night from sum equations, e.g., for the y -filter

$$\sum_n y_{obs} = nV_{std} + n\alpha_y(v - y) + \beta_y \sum_n (X - 1) + \gamma_y \sum_n T + n\delta_y \quad (8)$$

which was solved for y_{std} and v_{std} . These values were used to transform the individual measurements in each filter so that outlying measurements could be discarded before calculating the nightly mean for a given star. The individual measurements in each filter were used for calculating the uncertainty of the mean. This

procedure was then repeated for the other filters. The standard $uvby - \beta$ magnitudes were calculated as weighted means of the measurements from the first and the second night. The mean differences between the magnitudes measured on the two nights were smaller than 0.01 mag in all cases and typically equal to few mmag for stars brighter than $V=15$ mag.

In Table 3, we give the equatorial coordinates, the standard $uvby - \beta$ magnitudes, and the m_1 and c_1 Strömrgren indices for each star. We use values greater than 50 to code those β measurements which were measured on one night only and are uncertain. The code '0.000' is used for those uncertainties of individual $uvby$ magnitudes which were derived from one or two individual points, which is not enough to determine the standard deviation. The code '99.999' is used for magnitudes which were not measured. The full table is available in the electronic form from the Acta Astronomica Archive (see the cover page). A sample, containing the heading and the $uvby - \beta$ magnitudes from the first five rows and the last row, is printed below.

Table 3

A sample of the $uvby - \beta$ photometry of stars in NGC 7062.

ID	α_{2000}	δ_{2000}	y	b	v	u	β
1	21:23:19.4	46:20:23.4	16.066	16.937	18.131	19.832	2.621
2	21:23:30.4	46:20:23.3	18.564	19.772	21.244	23.198	2.649
3	21:23:24.8	46:20:24.0	18.228	18.951	19.925	21.220	2.479
4	21:23:30.1	46:20:23.8	14.740	16.075	18.143	20.640	2.617
5	21:23:44.0	46:20:22.6	20.329	21.054	22.037	22.654	51.287
...
904	21 23 34.30	46 26 40.90	99.999	99.999	21.900	99.999	99.999

In Fig. 1, we plot the color-magnitude diagram for stars in the field of NGC 7062. We use circles to indicate variable stars which we discuss in Sect. 3.

As the precision of our photometry drops for stars fainter than $V = 18$ mag, for computing the color excess of NGC 7062 we used only main-sequence stars brighter than this limit. We de-reddened each star by means of the method of Crawford (1979) and computed a weighed mean $E(B - V) = 0.43 \pm 0.05$ mag. Then, we compared the $(b - y) - c_1$ diagrams constructed for NGC 7062 and for M 11 (=NGC 6705). For the latter cluster, whose $E(B - V) = 0.428 \pm 0.027$ (see Sung et al. 1999), we used existing but unpublished Strömrgren photometry obtained by F.G. We found that the difference of the color excess between these two clusters is smaller than 0.04 mag and hence the two values agree with each other to within the one standard deviation. Therefore, we adopt $E(B - V) = 0.43$ as the color excess of NGC 7062.

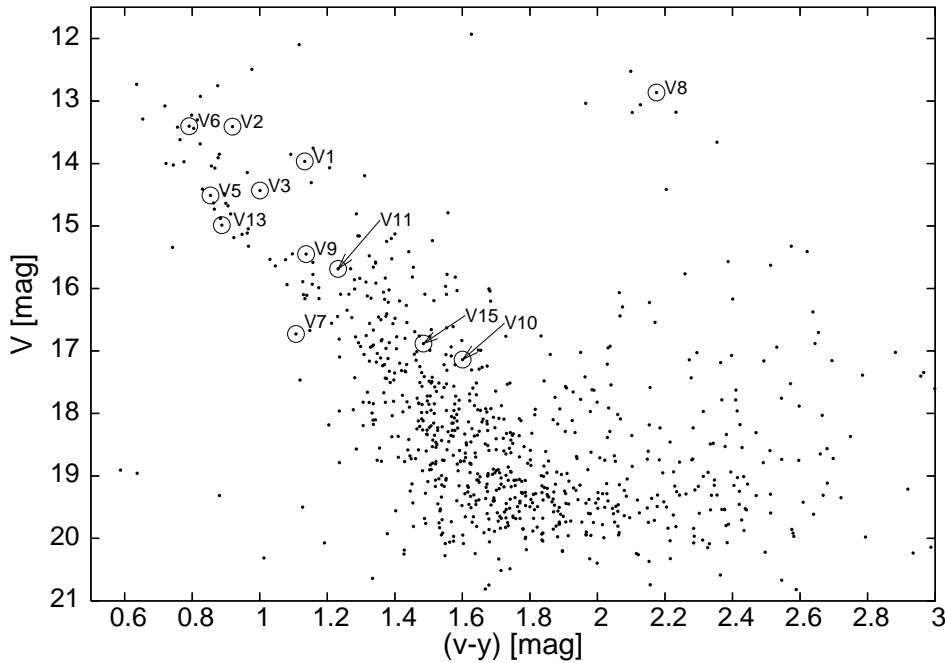


Fig. 1. Color - magnitude diagram for stars observed in the open cluster NGC 7062 and listed in Table 3. Variable stars are indicated with circles.

A similar comparison of $(v-y) - V$ and $c_1 - V$ diagrams constructed for these two clusters (not shown) yields a difference in the distance modulus between M 11 and NGC 7062 equal to -0.2 mag, which places NGC 7062 0.2 mag closer than M 11. Sung et al. (1999) provide a distance modulus of M 11, $V_0 - M_V = 11.55 \pm 0.1$, which corresponds to an apparent distance modulus of 12.92 for that cluster and thus results in 12.72 for NGC 7062. The last value is in a good agreement with 12.76 ± 0.4 given by Freyhammer et al. (2001).

2.2. Spectroscopy of NGC 1817 and NGC 7062

The spectroscopic observations were carried out at the Nordic Optical Telescope by S. F. (13–14 August 2004), and by T. A. and J. M.–Ž. (20–22 November 2004). The Andalucia Faint Object Spectrograph and Camera, ALFOSC, was used on both observing runs. The ALFOSC setup consisted of grism 9 working in the echelle mode and grism 11 working as a cross-disperser. A 2048×2048 px NIMO Back Illuminated CCD42-40 was used as the detector. The total wavelength range of the spectrograms was 3900–10350Å and their resolution ranged from 4500 at 5000Å to 3900 at 7500Å.

The list of targets included eleven stars in NGC 1817 and three in NGC 7062. The typical exposure time was 1800 s, which resulted in a signal-to-noise ratio of around 60 for most stars. The data were reduced with the IRAF² software, and the

²IRAF is distributed by the National Optical Astronomy Observatories, which are operated by the

spectra were extracted with the `apall` task also provided by IRAF. We give the log of our spectroscopic observations in Table 6.

3. Effective Temperature and Surface Gravity

3.1. From Strömgren indices

We derived the effective temperature and surface gravity of stars in NGC 7062 and NGC 1817 using Strömgren indices from our Table 3 and from Balaguer-Núñez et al. (2004), respectively. For the computations, we used the calibration of Napiwotzki et al. (1993) and the code kindly provided by the authors. We give the values of T_{eff} and $\log g$ in Table 4 (columns headed ‘observations’) together with standard deviations calculated from observational errors of the Strömgren indices β and c_0 . The large dispersion of $\sigma_{T_{\text{eff}}}$ for stars in NGC 1817 results from the very high dispersion of σ_{β} given by Balaguer-Núñez et al. (2004), which can vary by a factor of 20 from star to star.

Comparing the values of $\log g$ given by Balaguer-Núñez et al. (2004) for stars in NGC 1817 with those listed in Table 4, we find a satisfactory agreement. Unfortunately, such an agreement does not exist for the effective temperatures and absolute magnitudes, as the stars discussed by Balaguer-Núñez et al. (2004) are found to be cooler and brighter than in this paper. We discuss these discrepancies in more detail in the Appendix.

3.2. From 2MASS photometry

We compared the values of T_{eff} derived from Strömgren indices with those resulting from 2MASS indices ($V - J$), ($V - H$) and ($V - K$). For these computations we used the calibration of Kinman & Castelli (2002). For NGC 1817, we adopted $E(B - V) = 0.28$ from Balaguer-Núñez et al. (2004), for NGC 7062, $E(B - V) = 0.430$ from this paper. We de-reddened the 2MASS magnitudes using the $A(\lambda)/E(B - V)$ ratios provided by Cutri et al. (2003) and transformed the de-reddened magnitudes to the Bessell & Brett (1988) homogenized system. For NGC 1817 we adopted $[\text{Fe}/\text{H}] = -0.30$, which is a mean of the $[\text{Fe}/\text{H}]$ determinations from the literature that range from -0.42 (Taylor 2001) to -0.26 (Twarog et al. 1997). For NGC 7062, we used $[\text{Fe}/\text{H}] = -0.35$ as derived by Peniche et al. (1990) from photometry. The values of $\log g$ which are required by the calibration of Kinman & Castelli (2002) were adopted from Table 4 (the columns headed ‘observations.’)

The effective temperatures derived from the three color indices are given in Table 5. This table does not list NGC 7062–V7 and –V8, which are too hot for the calibration, NGC 7062–V11 and –V13, for which 2MASS magnitudes are of low quality (the 2MASS quality flag, `Qflag`, set to ‘E’), and NGC 7062–V15, which

Table 4

Variable stars in NGC 1817 and NGC 7062 from Arentoft et al. (2005) and Freyhammer et al. (2001), respectively. BN04 refers to the identification number from Balaguer-Núñez et al. (2004), ID, to the number from Table 3. The effective temperature and gravity computed from Strömgren indices and model atmospheres are given in the columns headed 'observations' and 'models'.

NGC 1817									
star	BN04	V	α_{2000}	δ_{2000}	$T_{\text{eff}} \pm \sigma$	$\log g \pm \sigma$	T_{eff}	$\log g$	
					observations		models		
V1	167	13.53	05 12 42.8	+16 41 43	7991±434	3.96±0.06	7750	4.0	
V2	154	12.88	05 12 40.8	+16 42 00	7298±317	3.50±0.06	7250	3.5	
V3	184	14.42	05 12 37.4	+16 42 31	7962±707	4.49±0.02	7750	4.5	
V4	7615	12.62	05 12 32.3	+16 44 52	7095±264	3.66±0.15	7000	3.5	
V6	156	12.95	05 12 33.1	+16 41 50	7648±700	4.14±0.05	8000	4.5	
V7	7632	13.73	05 12 40.1	+16 46 07	7521±527	3.94±0.15	7500	4.0	
V8	423	14.37	05 12 33.7	+16 43 22	6968±816	4.07±0.17	7250	4.5	
V9	7294	13.18	05 12 24.6	+16 43 32	6893± 38	3.57±0.16	7250	4.0	
V11	7097	14.32	05 12 30.4	+16 41 29	8075±589	4.65±0.09	8250	5.0	
V12	7105	14.71	05 12 27.9	+16 40 06	7333±174	4.60±0.13	7250	4.5	
V18	7145	14.24	05 12 30.0	+16 37 30	7091± 98	4.12±0.11	7000	4.0	
NGC 7062									
star	ID	V	α_{2000}	δ_{2000}	$T_{\text{eff}} \pm \sigma$	$\log g \pm \sigma$	T_{eff}	$\log g$	
					observations		models		
V1	357	13.97	21 23 29.8	+46 22 38	7749±185	4.20±0.02	7750	4.5	
V2	184	13.41	21 23 30.5	+46 21 38	8074±193	3.54±0.02	8000	3.5	
V3	594	14.43	21 23 35.8	+46 24 10	7945±345	3.91±0.03	8000	4.0	
V5	728	14.51	21 23 21.7	+46 25 12	8218±282	3.91±0.04	8000	4.0	
V6	396	13.40	21 23 21.5	+46 22 59	8500±347	4.05±0.04	8250	4.0	
V7	836	16.73	21 23 46.3	+46 26 00	9577±218	3.54±0.40	9750	4.5	
V8	69	12.86	21 23 13.6	+46 20 51	14812±235	2.49±0.02	14000	2.0	
V9	562	15.45	21 23 40.1	+46 23 56	7694±490	4.40±0.06	7500	4.5	
V10	328	17.14	21 23 22.9	+46 22 25	7906±594	4.19±0.09	8000	4.5	
V11	270	15.69	21 23 33.4	+46 22 07	7526±509	4.60±0.07	7250	4.5	
V13	145	14.99	21 23 18.5	+46 21 23	8235±265	3.93±0.12	8250	4.0	
V15	395	16.88	21 23 23.8	+46 22 58	7035±587	5.21±0.17	6750	5.0	

is too faint for the 2MASS Catalogue. The standard deviations of T_{eff} include photometric errors and the uncertainty of $\log g$ from Table 4.

In Fig. 2, we show the differences between T_{eff} obtained from the calibration of Napiwotzki et al. (1993) and those from the calibration of Kinman & Castelli (2002). The differences are positive for stars hotter than about 8000 K and negative, for the cooler. This trend is present for T_{eff} derived from each 2MASS photometric index and is most clearly visible in $(V - J)$, in which the maximum difference in

Table 5

Atmospheric parameters determined from *JHK* indices for stars in NGC 1817 and NGC 7062.

NGC 1817				
star	2MASS ID	$T_{\text{eff}}^{V-J} \pm \sigma$	$T_{\text{eff}}^{V-H} \pm \sigma$	$T_{\text{eff}}^{V-K} \pm \sigma$
V1	05124282+1641432	8118±61	8044±58	8037±65
V2	05124081+1642003	7970±50	7858±45	7784±55
V3	05123739+1642308	7982±26	7839±41	7722±60
V4	05123227+1644518	7956±49	7815±47	7813±54
V6	05123307+1641503	7963±30	7827±40	7721±47
V7	05124010+1646072	8224±80	8105±68	8213±92
V8	05123370+1643220	7917±37	7717±63	7658±71
V9	05122460+1643324	7882±39	7664±47	7595±47
V11	05123036+1641285	8091±47	7929±43	7782±54
V12	05122787+1640062	7959±26	7658±57	7500±69
V18	05122997+1637296	7961±37	7814±39	7687±48
NGC 7062				
star	2MASS ID	$T_{\text{eff}}^{V-J} \pm \sigma$	$T_{\text{eff}}^{V-H} \pm \sigma$	$T_{\text{eff}}^{V-K} \pm \sigma$
V1	21232977+4622378	7988 ± 25	7834 ± 30	7783 ± 35
V2	21233057+4621376	7916 ± 27	7757 ± 28	7720 ± 30
V3	21233583+4624102	7993 ± 33	7807 ± 32	7743 ± 41
V5	21232168+4625115	7903 ± 13	7769 ± 32	7650 ± 56
V6	21232154+4622592	8126 ± 49	8032 ± 42	7971 ± 43
V9	21234015+4623555	7839 ± 41	7225 ± 144	6704 ± 226
V10	21232292+4622246	8179 ± 79	7974 ± 75	7890 ± 144

T_{eff} computed for NGC 1817–V9 reaches 1000 K. The existence of this trend was not expected as no such feature is present in the comparison of T_{eff} derived by Kinman & Castelli (2002) from their calibration and by means of other methods.

3.3. From model atmospheres

We derived the effective temperature and surface gravity of the program stars using Kurucz ODFNEW model atmospheres³ computed for $[M/H] = 0.0$ and -0.5 , with the step in T_{eff} and $\log g$ equal to 250 K and 0.5 dex, respectively (Castelli & Kurucz 2004, Castelli & Kurucz 2006). In Table 4 (columns headed ‘models’), we give T_{eff} and $\log g$ of the model atmosphere of $[M/H] = 0.0$, for which the synthetic Strömgren indices are closest to the observed ones. For models computed for $[M/H] = -0.5$, either the resulting values of T_{eff} and $\log g$ were the same or no match was found.

In Fig. 3, we plot the differences between T_{eff} derived from the calibration

³available at <http://kurucz.harvard.edu/>

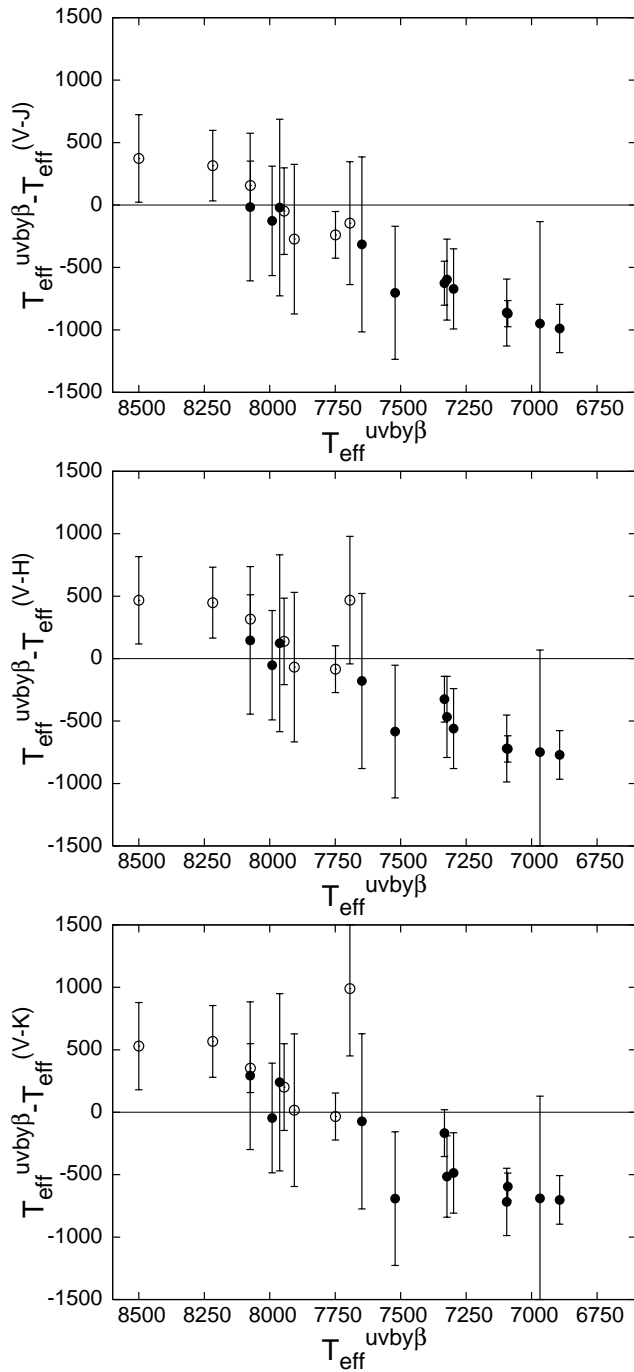


Fig. 2. Differences between T_{eff} computed from Strömrgren and 2MASS indices. Dots indicate stars in NGC 1817, open circles, stars in NGC 7062.

of Napiwotzki et al. (1993) and those derived from the model atmospheres. The

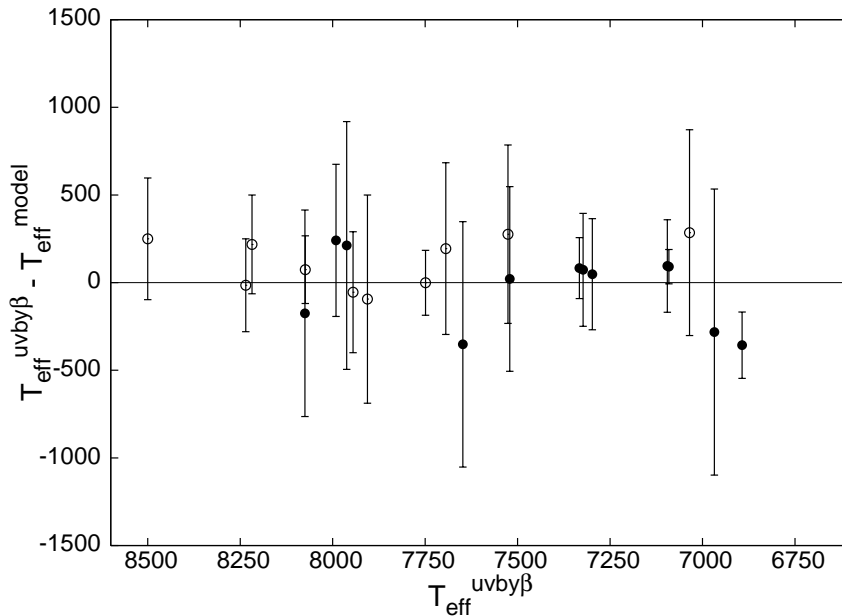


Fig. 3. Differences between T_{eff} computed from Strömgren indices and model atmospheres. Dots indicate stars in NGC 1817, open circles, stars in NGC 7062.

values agree well to within one standard deviation in all but one case and no trend is present. Having reached this consistency, we use the T_{eff} and $\log g$ obtained from the calibration of Napiwotzki et al. (1993) in the next steps of our analysis.

4. Radial Velocity and the Projected Rotational Velocity

The observed spectra with the ALFOSC instrument at the NOT have rather low resolution for detailed studies of radial and rotational velocities. But even with an instrumental width of the order 50 km/s one can still classify stars as fast or slow rotators or as binary stars.

We measured the radial velocity, RV , and $v \sin i$ of the program stars using two methods. First, we used the cross-correlation method and the `fxcor` task provided by IRAF. We obtained RV measurements in each order of the spectrograms and then computed the weighted mean RV . As templates, we used synthetic spectra computed from Kurucz ODFNEW model atmospheres. We used the ATLAS9 and SYNTHE (Sbordone et al. 2004, Sbordone 2005) software to compute the dedicated model atmosphere and the synthetic template spectrum for each program star for T_{eff} and $\log g$ adopted from Table 4 (columns headed 'observations') and $[\text{Fe}/\text{H}]$ equal to -0.30 and -0.35 for NGC 1817 and NGC 7062, respectively.

The projected rotational velocity was derived by comparing the observed spectrum with the synthetic one. The synthetic spectrum was rotationally broadened in a wide range of $v \sin i$ according to the formula provided by Gray (1992). Since the

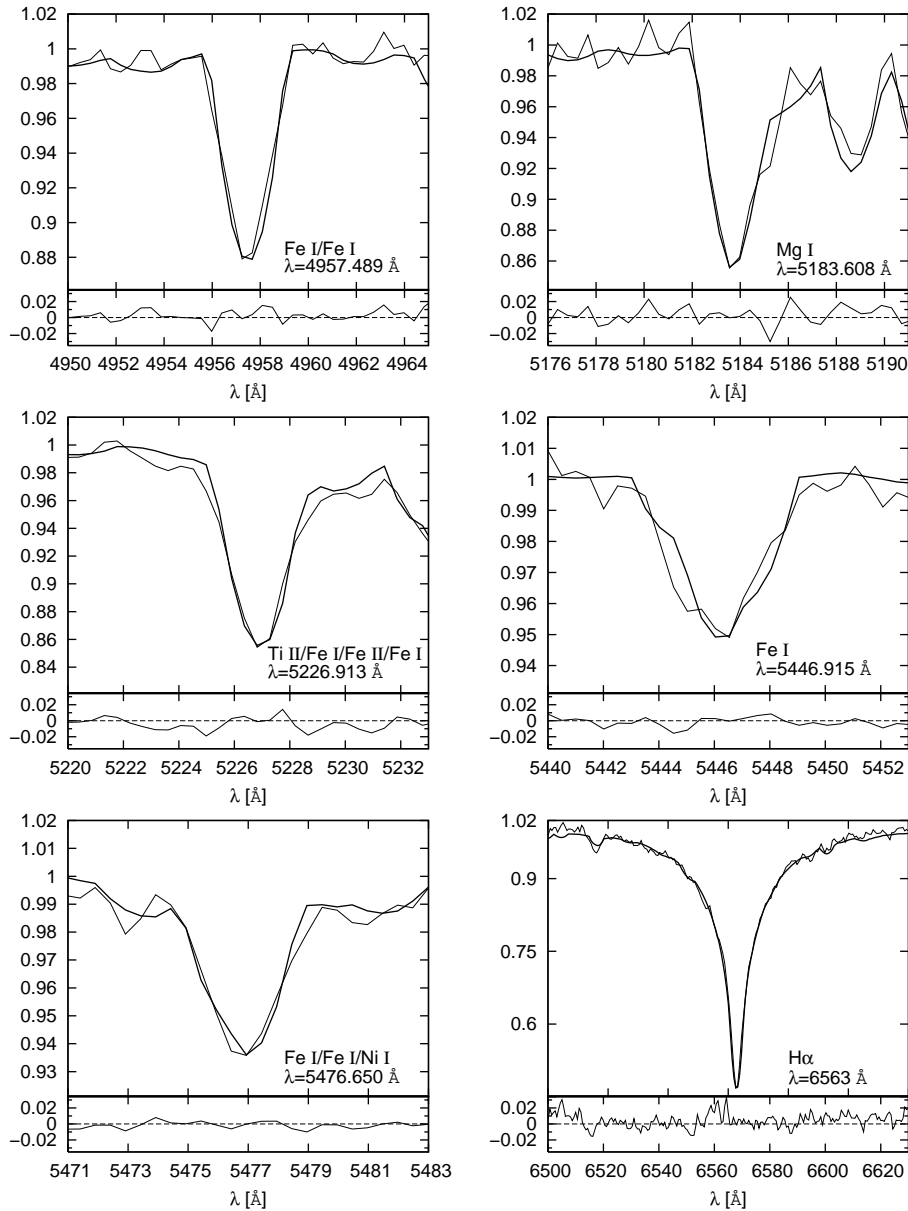


Fig. 4. The observed (thin line) and fitted spectrum (thick line), and the residuals of the fit calculated for six lines in NGC 1817–V2.

spectrograms measured by us have relatively low S/N ratios and most of our targets turned out to be fast rotators, the precise measurements of RV were difficult; the spectral lines were blurred and merged which caused problems with fitting the continuum and for determining whether the spectra correspond to single or multiple stars. For these reasons, we used mainly strong hydrogen lines but the metallic lines from Table 3 of Rasmussen et al. (2002) were used whenever possible. In

Fig. 4, we show fragments of the observed spectrum of NGC 1817–V2, one of our brightest targets, over-plotted with the fitted synthetic spectrum. At the bottom of each panel of the figure we show the residuals of the fit.

In the second method, we calculated broadening functions as described by Ruciński (1999), again using the synthetic spectra as templates. The broadening functions were computed individually for each echelle order and then a weighted average was formed. The weights were based on the deviation of each broadening function from the average. Finally, the rotational velocity and the barycentric radial velocity were derived by fitting a convolution of a Gaussian instrumental broadening and a rotational profile to the observed broadening function. The baseline and the amplitudes were kept fixed. For the binary stars, or for stars that might be binaries according to the shape of the broadening function, we fit two components. This was difficult because the components overlap and, as the broadening function has some noise peaks, these can be misinterpreted as a stellar component. We kept in mind, however, that if a binary star spectrum is assumed to come from a single star, it is possible to measure an artificially large $v \sin i$. In conclusion, we found that a significant fraction of the stars have broad profiles and that they clearly rotate at rather high rates.

In Fig. 5, we show the broadening functions calculated for ten δ Scuti stars in NGC 1817 and the eclipsing binary, NGC 1817–V18. The broadening functions for stars in NGC 7062 (not shown) look similar. Each panel of Fig. 5 is labeled with the number of the variable and shows several broadening functions shifted slightly upwards one with respect to another for the sake of clarity of the diagram. For four stars, we use thick lines to show the quality of the fitted curves. The broadening functions of the spectroscopic binaries, V01, V04 and V18, are clearly variable.

In Table 6, we list the RV computed with the use of the methods described above. The values range from 20 to 80 km/s; this dispersion is much larger than for open clusters in general but still not large enough that the membership to the cluster is ruled out for any of the stars. We suspect that the instrumental drift of the order 10 km/s might account for some of this dispersion.

Four stars from the studied sample show significant variability in radial velocity. Three of them, NGC 1817–V1, –V18, and NGC 7062–V1, we classify as single-lined spectroscopic binaries, and one, NGC 1817–V4, which was discovered to be an eclipsing binary by Arentoft et al. (2005), as a new spectroscopic double-lined binary. The latter classification was done on the basis of the shape of the broadening function. A few of the remaining stars also show indications of variability, but the uncertainties of the RV measurements are large and do not allow drawing firm conclusions.

In the second column of Table 6, we give the $v \sin i$ calculated as a mean of the values obtained from all examined spectral lines. The measured values range from 45 to 225 km/s for NGC 1817, and from 84 to 175 km/s for NGC 7062. The mean $v \sin i$ of δ Scuti stars in these two clusters are equal to 145 ± 21 and 116 ± 29 km/s,

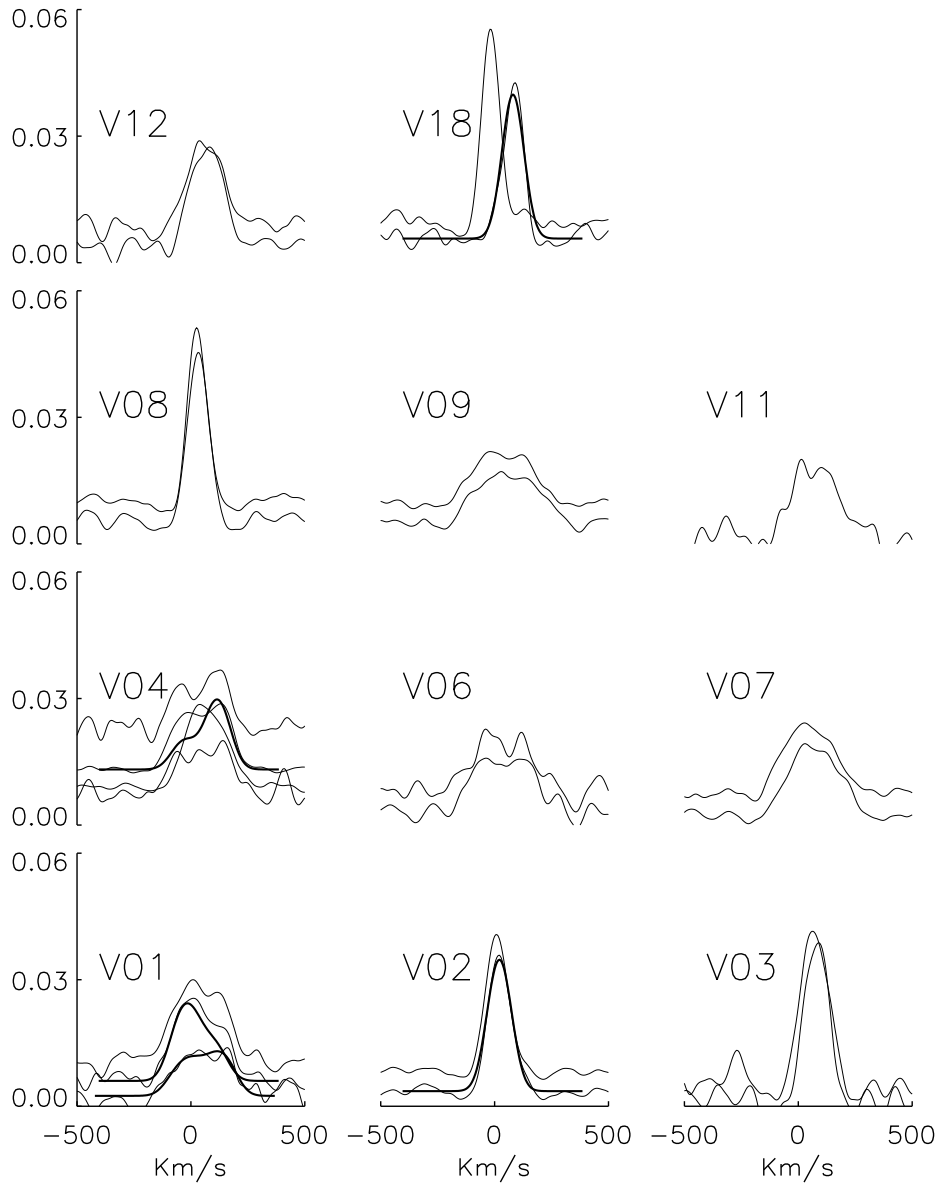


Fig. 5. The broadening functions for δ Sct stars and the SB1 eclipsing binary V18 in NGC 1817.

respectively. These numbers fall close to the median $v \sin i$ of δ Scuti stars in the Hyades cluster and in NGC 6134 (see Table 7 of Rasmussen et al. 2002). This adds NGC 1817 and NGC 7062 to the list of clusters in which δ Scuti stars rotate fast. We note, however, that for NGC 7062 the mean $v \sin i$ was calculated from three stars only.

Finally, in Fig. 6, we show $H\alpha$ line of NGC 1817–V8 for which the discrepancies between the effective temperature determined from the Strömgen and 2MASS

Table 6

Logbook of observations of NGC 1817 and NGC 7062. The columns contain star designations from Arentoft et al. (2005) and Freyhammer et al. (2001) for NGC 1817 and NGC 7062, respectively, the projected rotational velocity, $v \sin i$, the Heliocentric Julian Date of the mid-exposure, the exposure time in seconds, and the radial velocity.

star	$v \sin i$ [km/s]	HJD -2450000	t_{exp} [s]	$V_r \pm \sigma$ [km/s]	star	$v \sin i$ [km/s]	HJD -2450000	t_{exp} [s]	$V_r \pm \sigma$ [km/s]
NGC 1817					NGC 7062				
V1	194	3232.7382	1200	98.6 13.3	V1	84	3231.4900	1800	-28.9 2.6
		3330.5414	1800	58.0 9.3			3231.5141	1800	-14.9 1.1
		3330.5671	1800	63.0 6.8			3232.5166	1800	-2.1 1.1
.....								
V2	60	3331.6481	1800	32.5 2.7	V3	175	3231.5744	1800	20.7 6.8
		3331.6721	1800	27.3 4.4			3231.5988	1800	25.1 6.1
.....								
V3	76	3331.7363	1800	86.4 4.2	V5	90	3231.6288	1800	-1.0 2.8
		3331.7602	1800	75.7 4.5			3231.6533	1800	-11.3 2.9
.....								
V4	167	3330.4666	1800	58.7 13.6					
		3331.5022	1800	57.1 10.7					
		3331.7056	1800	89.3 7.1					
		3332.5656	1800	67.7 7.8					
.....								
V6	225	3332.4422	1800	68.5 14.5					
		3332.4760	1800	57.3 12.9					
.....								
V7	177	3330.6640	1800	77.6 4.4					
		3330.6881	1800	66.4 6.0					
.....								
V8	50	3330.6031	1800	47.4 3.1					
		3330.6277	1800	42.6 2.0					
.....								
V9	222	3332.5102	1800	54.9 5.6					
		3332.5341	1800	44.3 4.0					
.....								
V11	164	3332.6331	2400	82.0 7.2					
.....								
V12	119	3332.6680	1800	74.3 3.7					
		3332.6919	1800	63.8 4.0					
.....								
V18	45	3330.7226	1800	99.4 5.5					
		3332.5986	1800	1.4 3.8					

indices are of the highest. The measured spectrum is over-plotted with two synthetic $H\alpha$ lines. The first, plotted with a solid line, computed for a model atmo-

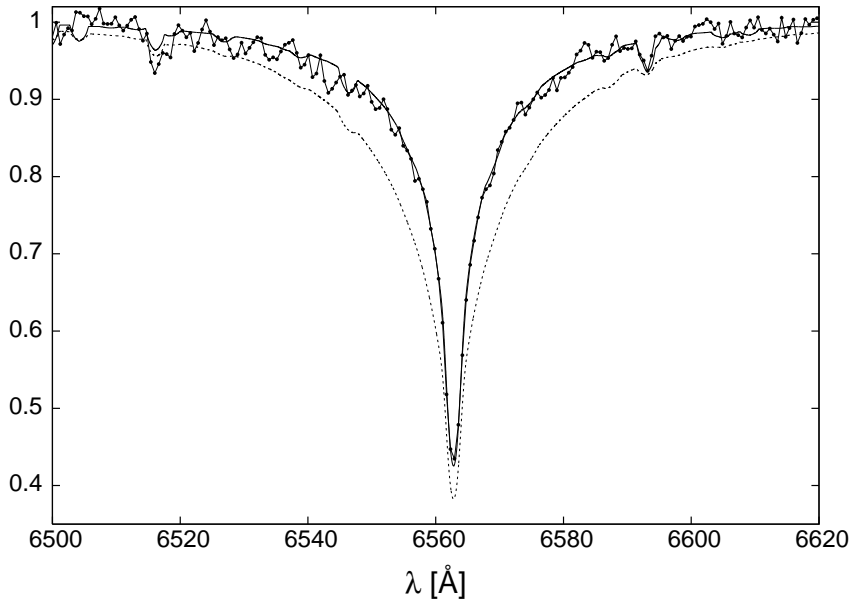


Fig. 6. NGC 1817-V8: the observed H α line over-plotted with two rotationally broadened synthetic H α lines computed for the same $\log g$ and two different T_{eff} (see the text).

sphere with $T_{\text{eff}} = 6968$ and $\log g = 4.07$ derived from Strömgen indices, and the second, plotted with a dashed line, for a model atmosphere with the same $\log g$ but $T_{\text{eff}} = 7250$ derived from $(V - J)$ index. Both synthetic spectra are rotationally broadened to 50 km/s. As can be seen, the synthetic spectrum computed for T_{eff} derived from $(V - J)$ index is substantially different from the observed one. For other stars with large differences in T_{eff} derived from Strömgen indices and 2MASS photometry, the discrepancies are similar. Therefore, we conclude that for stars discussed in this paper, atmospheric parameters obtained from Strömgen indices are more adequate, as they provide a better agreement between the observed and the computed spectra.

5. Summary

We reported results of spectroscopic and photometric observations of stars in NGC 1817 and NGC 7062, which were intended as preparation for a future multi-site asteroseismic campaign on δ Scuti stars in these clusters. The spectrograms were used for determination of the radial velocity and the projected rotational velocity of the program stars by means of two different methods.

NGC 1817-V1, -V18, and NGC 7062-V1 are discovered to be single-lined spectroscopic binaries, NGC 1817-V4, to be a double-lined spectroscopic binary, and all the observed stars are found to be moderate or fast rotators. The latter makes them challenging targets for asteroseismology as fast rotators are more complicated

to model (see, e.g., Kjeldsen et al. 1998), and their frequency spectrum is more difficult to interpret. We note, however, that there are successful attempts of asteroseismic analysis of rapidly rotating δ Scuti stars (see, e.g., Michel et al. 1999).

Acknowledgements. This publication makes use of data products from the Two Micron All Sky Survey, which is a joint project of the University of Massachusetts and the Infrared Processing and Analysis Center/California Institute of Technology, funded by the National Aeronautics and Space Administration and the National Science Foundation.

The data presented here have been taken using ALFOSC, which is owned by the Instituto de Astrofísica de Andalucía (IAA) and operated at the Nordic Optical Telescope under agreement between IAA and the NBIfAFG of the Astronomical Observatory of Copenhagen.

We made use of the SAO/NASA Astrophysics Data System (ADS) and the Asiago database on Photometric Systems (ADPS).

J.M.-Ž. and T.A. thank the Danish Natural Science Research Council for financial support. J.M.-Ž. acknowledges a partial financial support from the MNiSW grant N203 014 31/2650.

REFERENCES

- Arentoft, T., Bouzid, M.Y., Sterken, C., Freyhammer, L.M., and Frandsen, S. 2005, *PASP*, **117**, 601.
- Balaguer-Núñez L., Jordi C., Galadí-Enríquez D., and Masana E. 2004, *Astron. Astrophys.*, **426**, 827.
- Bessell, M.S., and Brett, J.M. 1988, *PASP*, **100**, 1134.
- Castelli, F., Kurucz, R.L. 2004, *Proc. IAU Symp. No 210, Modelling of Stellar Atmospheres*, eds. N. Piskunov et al., eprint arXiv:astro-ph/0405087.
- Castelli, F., Kurucz, R.L. 2006, *Astron. Astrophys.*, **454**, 333.
- Crawford D.L. 1979, *Astron. J.*, **84**, 1858.
- Cutri R.M. et al. 2003, *The 2MASS All-Sky Catalog of Point Sources, University of Massachusetts and Infrared Processing and Analysis Center IPAC/California Institute of Technology*.
- Flower P.J. 1996, *Astrophys. J.*, **469**, 355.
- Freyhammer, L.M., Arentoft, T., and Sterken, C. 2001, *Astron. Astrophys.*, **368**, 580.
- Gray, D.F. 1992, *The Observation and Analysis of Stellar Photospheres*, Cambridge University Press.
- Grundahl, F., Stetson, P.B., and Andersen, M.I. 2002, *Astron. Astrophys.*, **395**, 481.
- Kinman, T., and Castelli, F. 2002, *Astron. Astrophys.*, **391**, 1039.
- Kjeldsen, H., Arentoft, T., Bedding, T., Christensen-Dalsgaard, J., Frandsen, S., and Thompson, M.J. 1998, *Structure and Dynamics of the Interior of the Sun and Sun-like Stars SOHO 6/GONG 98, ESASP*, **418**, 385.
- Kjeldsen, H., and Frandsen, S. 1992, *PASP*, **104**, 413.
- Lang, K.R. 1992, *Astrophysical Data I. Planets and Stars, Springer-Verlag Berlin Heidelberg New York*.
- Masana, E., Jordi, C., and Ribas, I. 2006, *Astron. Astrophys.*, **450**, 735.
- Michel, E., Hernández, M.M., Houdek, G., Goupil, M.J., Lebreton, Y., Pérez Hernández, F., Baglin, A., Belmonte, J.A., and Soufi, F. 1999, *Astron. Astrophys.*, **342**, 153.
- Moon, T.T., and Dworetzky, M.M. 1985, *MNRAS*, **217**, 305.
- Napiwotzki, R., Schönberner, D., and Wenske, V. 1993, *Astron. Astrophys.*, **268**, 653.
- Olsen, E.H. 1983, *Astron. Astrophys. Suppl. Ser.*, **54**, 55.

- Olsen, E.H. 1984, *Astron. Astrophys. Suppl. Ser.*, **57**, 443.
- Peniche, R., Peña, J.H., Diaz-Martinez, S.H., and Gomez, T. 1990, *Rev. Mex. Astron. Astrofis.*, **20**, 127.
- Rasmussen, M.B., Bruntt, H. Frandsen, S., Pautzen, E., and Maitzen, H.M. 2002, *Astron. Astrophys.*, **390**, 109.
- Ruciński S.M. 1999, *IAU Coll. 170, "Precise Stellar Radial Velocities"*, Eds. Hearnshaw and Scarfe, *ASP Conf. Ser.*, **185**, 82.
- Sbordone, L. 2005, *Mem. Soc. Astron. Ital. Suppl.*, **8**, 61.
- Sbordone, L., Bonifacio, P., Castelli, F., and Kurucz, R.L. 2004, *Mem. Soc. Astron. Ital. Suppl.*, **5**, 93.
- Sung, H., Bessell, M.S., Lee, H.-W., Kang, Y.H., and Lee, S.-W. 1999, *MNRAS*, **310**, 982.
- Taylor, B.J. 2001, *Astron. Astrophys.*, **377**, 473.
- Twarog, B.A., Ashman, K.M., and Anthony-Twarog, B.J. 1997, *Astron. J.*, **114**, 2556.

Appendix I

Table 7

T_{eff} , R/R_{\odot} and M_V of four stars in NGC 1817 derived by Balaguer-Núñez et al. (2004) and in this paper, the absolute visual magnitude $M_V^{\log L}$ which results from the total luminosity of the star, and the difference $\Delta M_V = M_V^{\log L} - M_V$.

star	T_{eff}	R/R_{\odot}	M_V	$M_V^{\log L}$	ΔM_V	T_{eff}	R/R_{\odot}	M_V	$M_V^{\log L}$	ΔM_V
	Balaguer-Núñez et al. (2004)									
V1	7794	2.55	1.77	1.38	-0.39	7991	1.84	2.04	1.99	-0.05
V2	7105	4.61	0.57	0.49	-0.08	7298	3.63	0.84	0.89	0.05
V3	7731	1.37	3.30	2.76	-0.54	7962	1.01	3.49	3.31	-0.18
V4	6917	3.38	1.37	1.29	-0.08	7095	2.88	1.48	1.52	0.04

Balaguer-Núñez et al. (2004) compute atmospheric parameters of selected stars in NGC 1817 adopting $[\text{Fe}/\text{H}] = -0.34$ and using the grid of Moon & Dworetsky (1954) which they modify so that it is sensitive to the metallicity (unpublished). They derive the stellar effective temperature from the fit of the star’s flux to the synthetic spectra in four different bands (V-JHK) (Masana, private communication, see also Masana et al. 2006).

We find that the values of $\log g$ given by Balaguer-Núñez et al. (2004) agree well with those computed in this paper, but the effective temperatures are cooler and the absolute magnitudes, brighter. We illustrate these discrepancies in the top panel of Fig. 7 where we use circles for T_{eff} and M_V from Balaguer-Núñez et al. (2004) and dots, for this paper. Lines show mean $T_{\text{eff}}-M_V$ relations for dwarfs and giants from Lang (1992). Arrows join respective pairs of stars. The relevant values of T_{eff} and M_V are given in Table 7.

The discrepancies are opposite to what might be expected for metal-poor stars whose T_{eff} is determined from the β index. We illustrate this in the bottom panel of Fig. 7, where we plot the $T_{\text{eff}} - \beta$ relation for Kurucz ODFNEW model atmospheres computed for $\log g = 4.0$, and $[\text{M}/\text{H}] = 0.0$ (dashed line) and -0.5 (solid line). According to these models, of two stars that have the same β and $\log g$, the metal-deficient one should be hotter. As an example, we show that a star with $\log g = 4.0$, $\beta = 2.835$ and $[\text{M}/\text{H}] = 0.0$ should have $T_{\text{eff}} = 7742$ K (dashed arrow) while a star with the same $\log g$ and β but $[\text{M}/\text{H}] = -0.5$ should have $T_{\text{eff}} = 7795$ K, (solid arrow). As Balaguer-Núñez et al. (2004) do not use the β index for the determination of T_{eff} , the noticed discrepancies must result from differences in the calibrations of T_{eff} in Strömberg and JHK indices.

Considering the values of M_V listed by Balaguer-Núñez et al. (2004), we find

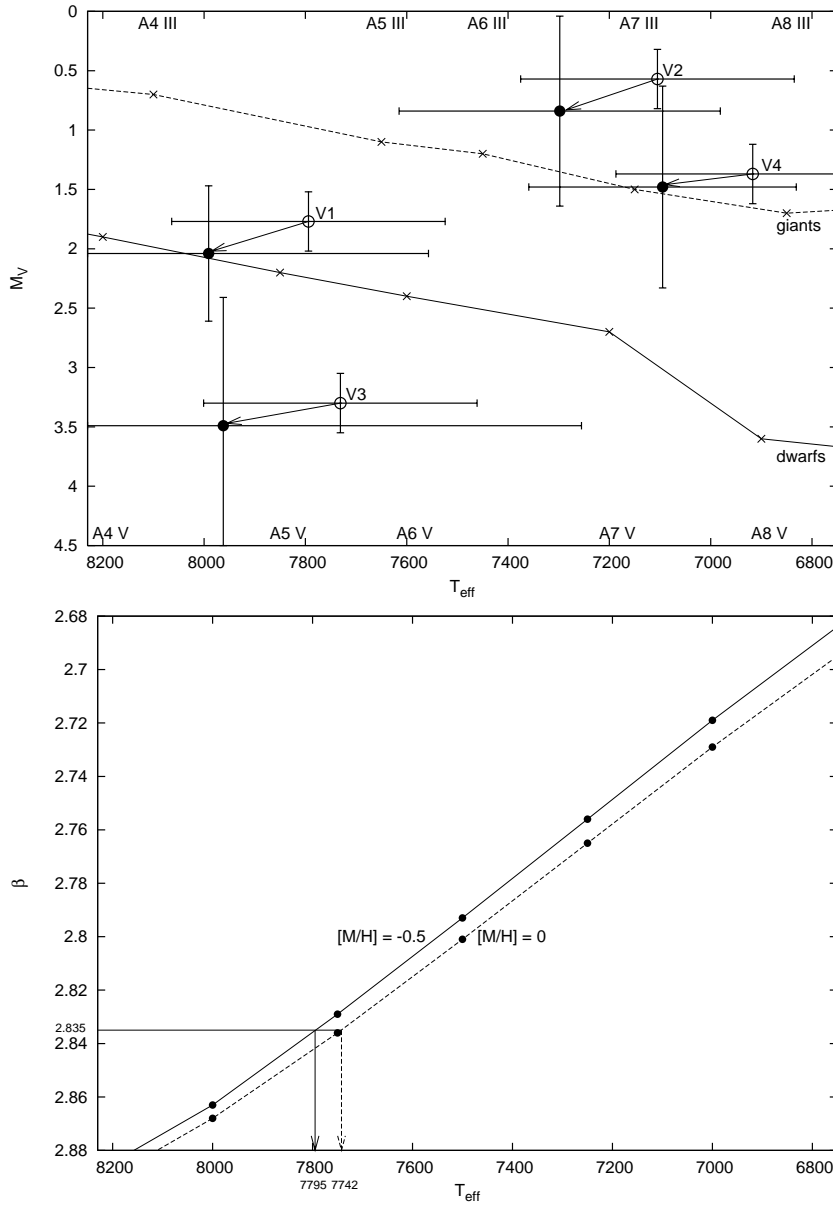


Fig. 7. *Top*: $T_{\text{eff}}-M_V$ diagram for stars in NGC 1817 discussed in this paper and in Balaguer-Núñez et al. (2004). *Bottom*: $T_{\text{eff}}-\beta$ relation for stars of different metallicities. Arrows show that for a fixed $\log g$ and β a metal-poor star is hotter than a star of solar metallicity.

that in some cases they are significantly different from $M_V^{\log L}$, the absolute magnitude which results from the total luminosity of the star

$$M_V^{\log L} = M_{\text{bol}} - BC \quad (9)$$

where

$$M_{\text{bol}} = -2.5 \log L/L_{\odot} + M_{\text{bol},\odot} \quad (10)$$

and

$$L = 4\pi R^2 \sigma T_{\text{eff}}^4 \quad (11)$$

In Table 7, we calculate the differences between $M_V^{\log L}$ and M_V using T_{eff} and R/R_{\odot} from Table 7 of Balaguer-Núñez et al. (2004) and the values derived in this paper. We used the bolometric correction, BC, from Flower (1996), the solar effective temperature, $T_{\text{eff},\odot} = 5778\text{K}$, and the solar bolometric absolute magnitude, $M_{\text{bol},\odot} = 4.75$ mag. We find that in all cases the consistency between $M_V^{\log L}$ and M_V is better for the calibration of Napiwotzki et al. (1993). Therefore, we suspect that the large values of ΔM_V found for Balaguer-Núñez et al. (2004) may indicate some problems with consistency of their calibration.